Delineating the Cellular Mechanisms Associated with Skin Electroporation

Katherine Schultheis,[1] Trevor R.F. Smith,[1] William B. Kiosses,[2] Kimberly A. Kraynyak,[1] Amelia Wong,[1] Janet Oh,[1] and Kate E. Broderick[1,*]

[1]Inovio Pharmaceuticals, Inc., Plymouth Meeting, Pennsylvania; [2]The Scripps Research Institute, Core Microscopy Facility, La Jolla, California.

The immune responses elicited following delivery of DNA vaccines to the skin has previously been shown to be significantly enhanced by the addition of electroporation (EP) to the treatment protocol. Principally, EP increases the transfection of plasmid DNA (pDNA) into the resident skin cells. In addition to increasing the levels of *in vivo* transfection, the physical insult induced by EP is associated with activation of innate pathways which are believed to mediate an adjuvant effect, further enhancing DNA vaccine responses. We investigated the possible mechanisms associated with this adjuvant effect, primarily focusing on the cell death pathways associated with the skin EP procedure independent of pDNA delivery. Using the minimally invasive CELLECTRA®-3P intradermal electroporation device that penetrates the epidermal and dermal layers of the skin, we have investigated apoptotic and necrotic cell death in relation to the vicinity of the electrode needles and electric field generated. Employing the well-established terminal deoxynucleotidyl transferase nick-end labeling assay, we detected apoptosis beginning as early as one hour after EP and peaking at the 4 h time point. The majority of the apoptotic events were detected in the epidermal region directly adjacent to the electrode needle. Using a novel propidium iodide *in vivo* necrotic cell death assay, we detected necrotic events concentrated in the epidermal region adjacent to the electrode. Furthermore, we detected upregulation of calreticulin expression on skin cells after EP, thus labeling these cells for uptake by dendritic cells and macrophages. These results allow us to delineate the cell death mechanisms occurring in the skin following intradermal EP independently of pDNA delivery. We believe these events contribute to the adjuvant effect observed following electroporation at the skin treatment site.

Keywords: electroporation, apoptosis, necrosis, skin

INTRODUCTION

THE DERMAL TISSUE is accessible and enriched in professional antigen presenting cells and therefore it offers an appropriate and attractive target for vaccination. Immunization in the skin elicits both T and B cell host immune responses in a dose-sparing fashion.[1] In multiple preclinical models, DNA vaccines have been successfully delivered to the skin to protect against a variety of infectious diseases, such as Ebola, Lassa, and influenza, and we have recently observed robust humoral and T cell responses in humans to Ebola and HIV antigens after intradermal (ID) delivery of a DNA vaccine (manuscripts in preparation).[2–4] As is the case with intramuscular DNA vaccine delivery, the physical delivery method of electroporation (EP) has been shown to significantly enhance the uptake of DNA to cells in the skin. DNA vaccine protocols, injected in either skin or muscle sites, which include EP have been associated with significantly augmented host immune responses against the expressed antigen.[4–10] In this study, we have focused our attention to the minimally invasive ID CELLECTRA®-3P (Inovio Pharmaceuticals, Plymouth Meeting, PA) constant current electroporation device, designed to maintain a square wave pulse form in the target tissue irrespective of changes in tissue resistance. This is especially advantageous in the dermal space due to the highly variable thickness and physiology of

*Correspondence: Dr. Kate E. Broderick, Inovio Pharmaceuticals, Inc., 660 W. Germantown Pike, Suite 110, Plymouth Meeting, PA 19462. E-mail: kate.broderick@inovio.com

DOI: 10.1089/hgtb.2017.105

human skin. Previous studies assessing a wide range of viral antigens after skin plasmid DNA (pDNA) vaccination with CELLECTRA®-3P have consistently shown robust immune responses in both guinea pigs and nonhuman primates.[5,11,12] Furthermore, due to the minimally invasive nature of this EP platform and the lower electrical parameters used compared with intramuscular EP, pain scores associated with skin EP have been reported to be significantly lower than those associated with muscle EP.[13] The CELLECTRA®-3P EP device is currently being employed in the clinic to deliver DNA-encoded vaccines against Ebola (NCT02464670), HIV (NCT02431767), and Zika (NCT02809443 and NCT02887482) to the skin.

The principal mechanism by which EP aides the augmentation of the immune response elicited by DNA vaccines is by significantly increasing the number of cells transfected by the plasmid in the target tissue of choice. This results in higher levels of gene expression, generally considered to be 100- to 1000-fold increased.[14] However, the increase in transfection rates are not the only *in vivo* mechanism mediated by EP. Others include inflammatory cell infiltration at the treatment site, cell death after antigen expression, and/or upregulation of inflammatory signals. While cell infiltration and upregulation of inflammatory signals may potentially enhance the host immune response elicited, cell death and decreased antigen expression may impede these responses.[8,15,16]

To facilitate a targeted approach of optimizing EP parameters toward immunogenicity, the adjuvant effect of EP by itself should be investigated independently from other aspects of the treatment, such as the introduction of exogenous DNA into the target tissue, and the subsequent expression and immunogenic nature of the antigen product. Delineating the direct impact of EP alone on these mechanisms can be difficult since the situation is complicated further by the synergist pro-inflammatory impact of the DNA vaccine. We believe a more complete understanding of the local physiological mechanisms specifically initiated after EP will provide us with a clearer understanding of the potential downstream effects on the immune response elicited after DNA vaccination. Here we describe the cellular events immediately following the physical impact of applying an electrical field to skin in an *in-vivo* model. This knowledge will aide in tailoring skin EP procedures and identify the optimal balance between skin damage that will promote productive host immune responses, and the possible mechanisms that could hinder this.

The study reported here has been performed in the Hartley guinea pig research model. This animal model represents an excellent surrogate for human skin in terms of its physiology and thickness, and aides the translation of the findings to the clinic. Previous studies focused on the delivery of reporter genes into the guinea pig skin with CELLECTRA®-3P, observed gene expression in the skin as early as one hour after delivery.[17] In these historical studies, we identified transfected cells in the epidermis, dermis, and subdermal regions following CELLECTRA®-3P EP. Here we have designed studies to understand the physiological consequences of the use of skin EP which could potentially impact gene expression and host immune responses. We investigated the localized tissue changes and inflammation resulting from CELLECTRA®-3P treatment of the skin. We used the terminal deoxynucleotidyl transferase nick-end labeling (TUNEL) assay and a novel propidium iodide (PI)–based assay to delineate the apoptotic and necrotic events, respectively. PI is impermeable to viable cells but can enter the cell and bind to the DNA when the plasma membrane integrity is compromised, whereby its fluorescence is enhanced by 20- to 30- fold. *In vivo* injection of PI has previously been used to visualize cerebral ischemia and infarct size measurement as well as intratumoral injection.[18–21] Whereas PI stains all cells with disrupted membrane integrity, representing necrotic cells, the TUNEL stain is specific for apoptotic DNA fragmentation, caused by the activation of endogenous endonucleases, specifically caspase-3 activated DNases. The TUNEL stain depends on free 3′-OH termini in DNA strand breaks. Furthermore, we investigated the kinetics of the infiltration of innate immune cells into the treatment site and *in situ* up-regulation of inflammatory signals. Finally we discuss the potential of the inflammatory mechanisms induced by EP to augment or hinder the host immune response generated.

MATERIALS AND METHODS

Animals and treatment

Female Hartley guinea pigs (Charles River) were 13 months of age when they entered this study. Animals were group housed (3 per cage) with *ad libidum* access to water and food. All animals were housed and handled according to the standards and protocols of the Institutional Animal Care and Use Committee at BTS, Inc. (San Diego, CA). Prior to the EP treatment, the abdominal flank was shaved and depilated. Phosphate-buffered saline (PBS; 100 μL) was injected at each treatment site using the Mantoux method for intradermal

injections, immediately followed by electroporation using the CELLECTRA®-3P device.

Electroporation treatment with the CELLECTRA®-3P

The CELLECTRA® pulse generator was set to maintain a constant current of 0.2 Amps. The intradermal 3P array consists of three needles orientated as depicted in Fig. 1A. It delivers two sets of pulses with a delay of 3 seconds between the first and second set. Within each set there are two 52 ms pulses with a 198 ms delay between the pulses. All experiments reported in this study were performed with the CELLECTRA®-3P in the guinea pig skin using the electrical parameters and pulse pattern described above.

Tissue processing and hematoxylin and eosin stain

Skin biopsies were excised postmortem at different time points (1 h, 2 h, 4 h, 6 h and 24 h) after the EP treatment. Biopsies were immersed in 4% paraformaldehyde (PFA) (ElectronMicroscopySciences, Hatfield, PA) in PBS for 12 h at 4°C. After washing biopsies (three times for 5 min with PBS), they were immersed in 30% (w/v) Sucrose (Sigma, St. Louis, MO) in D.I. water. Biopsies were molded in O.C.T. compound (Sakura, Torrance, CA) and snap-frozen at –80°C. Fixed and frozen skin samples were sectioned using an OTF Bright Cryostat (Hacker Instruments, Winnsboro, SC) to a thickness of 15 μm. Sections were stained using a regressive hematoxylin/eosin (H&E) stain (BBC Biochemical, Mount Vernon, WA), mounted with Permount (Fisher Chemical, Waltham, MA).

Propidium iodide *in vivo* injection

Propidium iodide *in vivo* injection at the treatment site in the skin was performed to measure cell death after electroporation. 50 μL of 10 μg/ml PI (Sigma) in PBS was injected at the EP treatment site using the Mantoux injection technique at indicated time points after EP. The guinea pig was sacrificed 20 minutes later according to standard institutional protocol. Twenty minutes was determined to be the optimal time for PI to enter damaged cells and bind to DNA, while remaining extracellular PI was diluted out by hydrostatic and osmotic pressure in the interstitial fluid. The harvested skin was put on ice for transport. The PI signal on the skin surface was imaged with an Olympus BX51 microscope with a Magnafire U-TVIX-2/U-CMAD 3 combo camera for photo acquisition (Olympus, New York, NY). Magnafire software was employed to acquire the images. Pixel count analysis was performed using the cell profiler software.[22]

In-situ TUNEL assay

Slides with PFA-fixed skin sections were incubated for 2 min in permeabilization solution (freshly

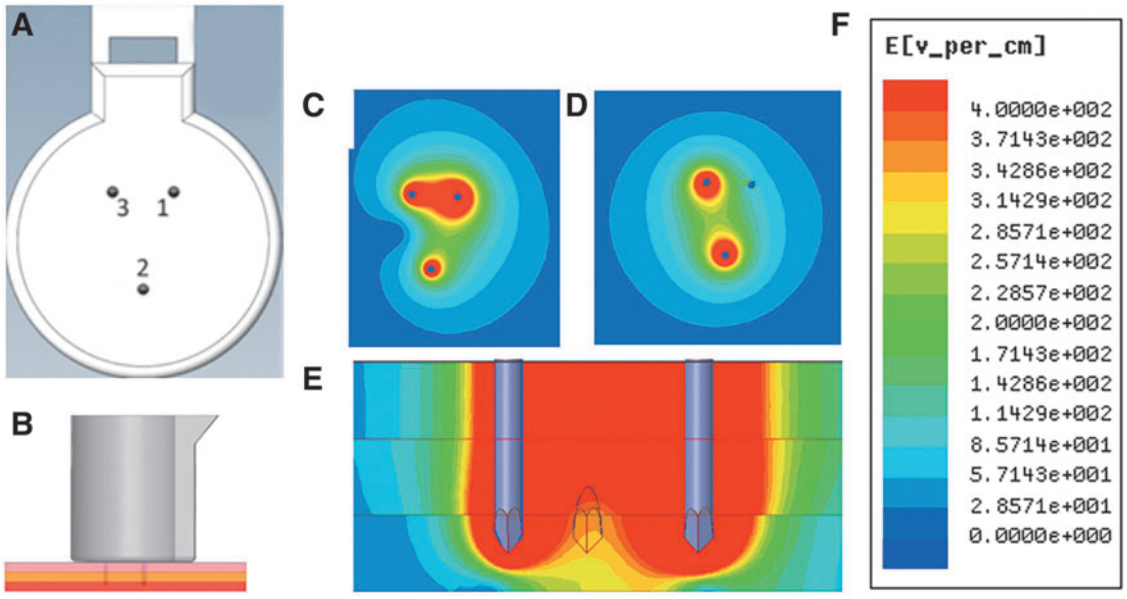

Figure 1. Physical and electrical characteristics of electroporation with the CELLECTRA®-3P device. Rendering of the face on view of the 3P intradermal electrode array **(A)**. Rendering of the lateral view of the array inserted into the skin (epidermis, pink; dermis, yellow; subdermal layers, red) **(B)**. Electrical-field generated by the CELLECTRA®-3P during the first pulse (face view) **(C)** and second pulse (face view) **(D)** and between electrodes 1 and 3 during the first pulse (lateral view) **(E)**. Strength of E-field (volts per cm) is color coded, with red for highest and blue for lowest field strength **(F)**. Images depicting the magnitude of the E-field were generated using the ANSYS Maxwell Finite Element Analysis software.

prepared 0.1% (v/v) Triton X-100 in 0.1% (w/v) sodium citrate). Slides were washed twice with 1×PBS for 5 min. 50 μL TUNEL reaction mixture (Roche, *In situ* cell death detection kit) was added per section, followed by incubation for 60 min at 37°C in a dark, humidified chamber. After washing slides three times for 5min with 1×PBS, sections were mounted with Fluoromount (Fisher). TUNEL-stain was imaged with a BX51 fluorescent microscope (Olympus) equipped with a Retiga3000 monochromatic camera (QImaging, Surrey, Canada). Where necessary, higher resolution images were acquired using a Zeiss LSM780 Laser Scanning Confocal Microscope (Carl Zeiss LLC, Jena, Germany) using a 63× objective. High resolution scanned images were collected from whole segments of dermis and autostitched with Zeiss tiling software into one large mega image, which was then further processed as maximum intensity projections, shown in Fig. 2.

Immunofluorescence detection of calreticulin

Fixed-frozen skin sections were incubated with 50 μL blocking buffer [0.3% (v/v) Triton-X (Sigma), 2% (v/v) donkey serum (Lampire Biological Laboratories, Ottsville, PA) in PBS] per section for 30 min at room temperature in a humidified chamber. Blocking buffer was gently tapped off. Polyclonal rabbit anti-human calreticulin antibody (ABIN361834, Antibodies-online) was diluted 1:100 in diluent buffer [1% (w/v) bovine serum albumen (Sigma), 2% (v/v) donkey serum, 0.3% (v/v) Triton-X (Sigma) and 0.025% (v/v) 1 g/mL NaN_3 (Sigma) in PBS]. Optimal dilution of the calreticulin antibody was determined on sections of guinea pig thyroid gland (data not shown). Fifty microliters of the staining solution was added to each section. Sections were incubated for 2 h at room temperature. Donkey anti-rabbit immunoglobulin G AF488 (A21206, life technologies, Waltham MA) was diluted 1:200 in diluent buffer. After washing the sections three times for 5 min in PBS, 50 μL of the secondary antibody solution was added per section. Sections were incubated 1hr at room temperature. Sections were mounted with DAPI (4′,6-diamidino-2-phenylindole)-Fluoromount (Southern Biotech, Birmingham AL). Calreticulin was imaged with a BX51 fluorescent microscope (Olympus) with a Retiga3000 monochromatic camera (QImaging).

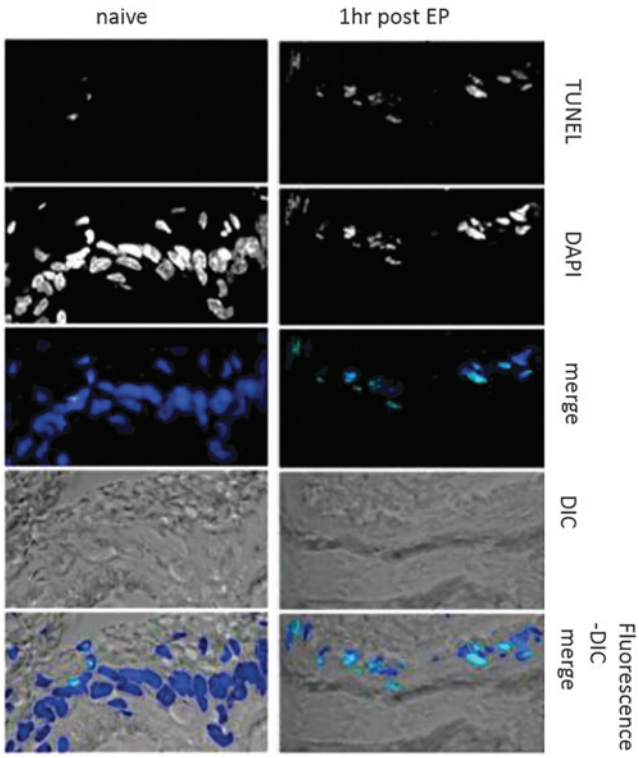

Figure 2. Cellular infiltration at the dermal electroporation site. Phospahate-buffered saline (PBS; 100 μL) was injected intradermally (Mantoux technique) into Hartley guinea pig skin CELLECTRA®-3P electroporation was immediately applied at the site of administration. Treatment site skin biopsies were harvested at the indicated time points, processed, sectioned, and stained with hematoxylin and eosin. Images shown are single representations for sections obtained from five treatment sites prior to treatment and at 1, 2, 4, 6, and 24 hours posttreatment.

RESULTS

The CELLECTRA®3P intradermal electroporation delivery device

The CELLECTRA®-3P is a minimally invasive intradermal clinical electroporation device which aides in the delivery of plasmid DNA to the skin. It is currently employed to enhance the delivery of DNA vaccines encoding Ebola, Zika, and HIV virus antigens in the clinic and we have reported increased tolerability of EP treatment at the skin with the CELLECTRA®-3P upon comparison to intramuscular electroporation.[13] The reduced insertion depth (3 mm) and the relatively mild EP electrical parameters compared with intramuscular EP are major contributors to the improved tolerability.

The electroporation array of the CELLECTRA®-3P consists of three solid stainless steel electrode needles. The needles are 3 mm in length and 26 Gauge. They form an isosceles triangle with a 5 mm distance from needle 1 to 2 and needle 2 to 3, and a 3 mm distance from needle 1 to 3 (Fig. 1A). When the electrode array is completely inserted at the treatment site, the electrode needles penetrate through epidermis and dermis (Fig. 1B). In the first pulse of each parameter set (Fig. 1C), needle 1 serves a cathode, and needles 2 and 3 as anodes. The second pulse in each parameter set (Fig. 1D) is between needle 2 (cathode) and needle 3 (anode). Using the ANSYS Maxwell Finite Element Analysis

software, the electrical (E)-field heat maps were generated to depict the electrical field strength for each pulse [pulse 1 (Fig. 1C) and pulse 2 (Fig. 1D)]. The lateral electrical field strength between electrodes 1 and 3 during the first pulse is depicted in Fig. 1E. The model predicts a field-strength of 400 V/cm adjacent to needles and weakens gradually toward the outer borders of the treatment site.

Cellular infiltration at the treatment site after ID electroporation

To model the kinetics of cellular infiltration in the skin at the CELLECTRA®-3P treatment site we performed H&E staining of tissue sections at time points between 0 to 24 hours after treatment (Fig. 2). Nuclei of all resident cells such as fibroblasts and motile immune cells stain dark violet following binding of basic hematoxylin to negatively charged nuclear DNA. The goal of this experiment was to observe the change in cell numbers after EP treatment. Such an observation would be indicative of infiltrating cells of the immune system, such as macrophages. Cellular infiltration to the treatment site was observed as early as two hours after EP treatment. Our time course suggested cellular infiltration peaked by 6 h after the treatment. The cellular infiltration at 24 hours was comparable to the level observed 6 h after treatment suggesting a plateau effect. In conclusion, the EP procedure caused a rapid influx of cells into the area of skin in close proximity to the treatment site. The level of infiltration was not as high as had previously been observed after the delivery of pDNA with CELLECTRA®-3P.[17] This suggested that the addition of pDNA in addition to the EP treatment further potentiated the influx of motile cells at the treatment site.

The images in Figure 2 are representative of skin areas directly within the EP treatment site and with a minimum distance of 1 mm from obvious histological needle marks. Disruption of the outer epithelial barriers of stratum corneum and epidermis was only observed at close proximity to the needle mark (within a 1 mm radius) and was significantly reduced 48 h after EP treatment (data not shown).

Intradermal electroporation induces rapid apoptotic events in the skin

To detect cell death following CELLECTRA®-3P electroporation in the skin, we performed TUNEL assay staining to detect apoptosis, which is associated with DNA fragmentation. Figure 3 compares apoptotic events occurring in the epidermis of untreated and treated skin one hour after EP. Low numbers of

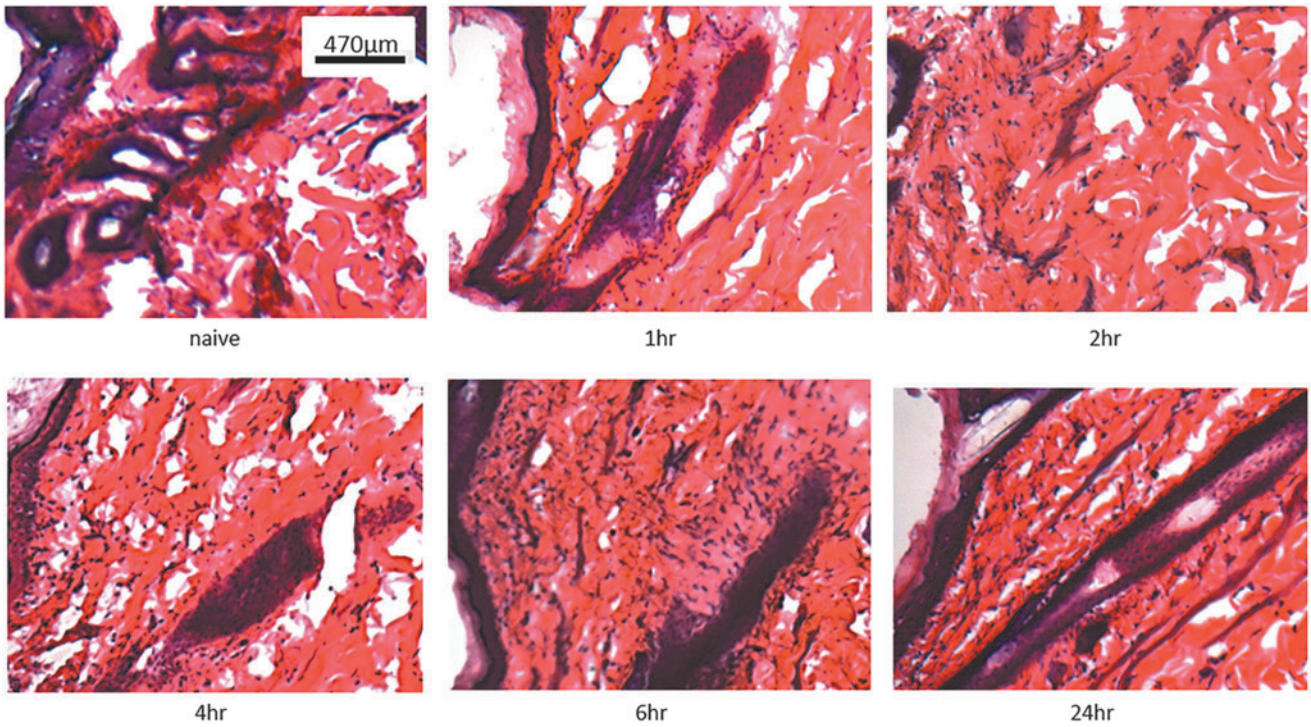

Figure 3. Dermal electroporation induces rapid apoptotic events. One hundred microliters of plasmid-encoded Red Fluorescent Protein (pRFP) (50 μg) was administered to guinea pig skin, and the site was immediately electroporated with the CELLECTRA®-3P (right panels); untreated skin is depicted in the left panels. Skin was harvested one hour after treatment and skin sections were stained with DAPI (blue) and TUNEL (green). DIC, differential interference contrast; DAPI, 4′,6-diamidino-2-phenylindole; TUNEL, terminal deoxynucleotidyl transferase nick-end labeling.

apoptotic TUNEL-positive cells were observed in the epidermis of untreated guinea pig skin (naive). One hour post EP treatment, the number of apoptotic cells in the epidermis was significantly increased along with pronounced disruption of the epidermal cellular structure in the region adjacent to the electrode insertion. The nuclei of cells in the EP–treated skin stained positive in a TUNEL assay to detect DNA strand breaks as a result of DNA fragmentation. Furthermore, the morphology of the cell nuclei in the treated sections had changed. TUNEL-positive nuclei appeared smaller which is likely due to the characteristic morphological changes associated with apoptosis which include nuclear fragmentation, degradation of the nuclear envelope, nuclear blebbing, and condensed DNA.

Intradermal electroporation induces necrotic events in the skin

We proceeded to analyze necrotic cell death in the EP-treated skin by injecting the fluorescent molecule propidium iodide (PI) into the treatment site at set time points after EP. PI binds to DNA by intercalating between the bases. It is membrane impermeable and excluded from viable cells or apoptotic cells with intact membranes. Thus the necrosis marker PI is commonly used to identify dead cells which have lost membrane integrity due to necrotic cell death. As expected, injection of the PI in untreated skin resulted in a negligible increase of the PI signal detected on the skin surface (Fig. 4A and B) upon comparison to skin sections without PI. Following EP treatment, the PI signal was significantly increased 1hr after treatment, and peaking around two hours after the treatment (Fig. 4A). At the 2-h time point, the isosceles triangular pattern of the 3P electrode needles insertion marks were visible in the areas of highest PI signal in the skin surface images (Fig. 4B). At 6 h after treatment the PI signal was decreased, and it has returned to background levels by 24 h after treatment. The detectable propidium iodide signal

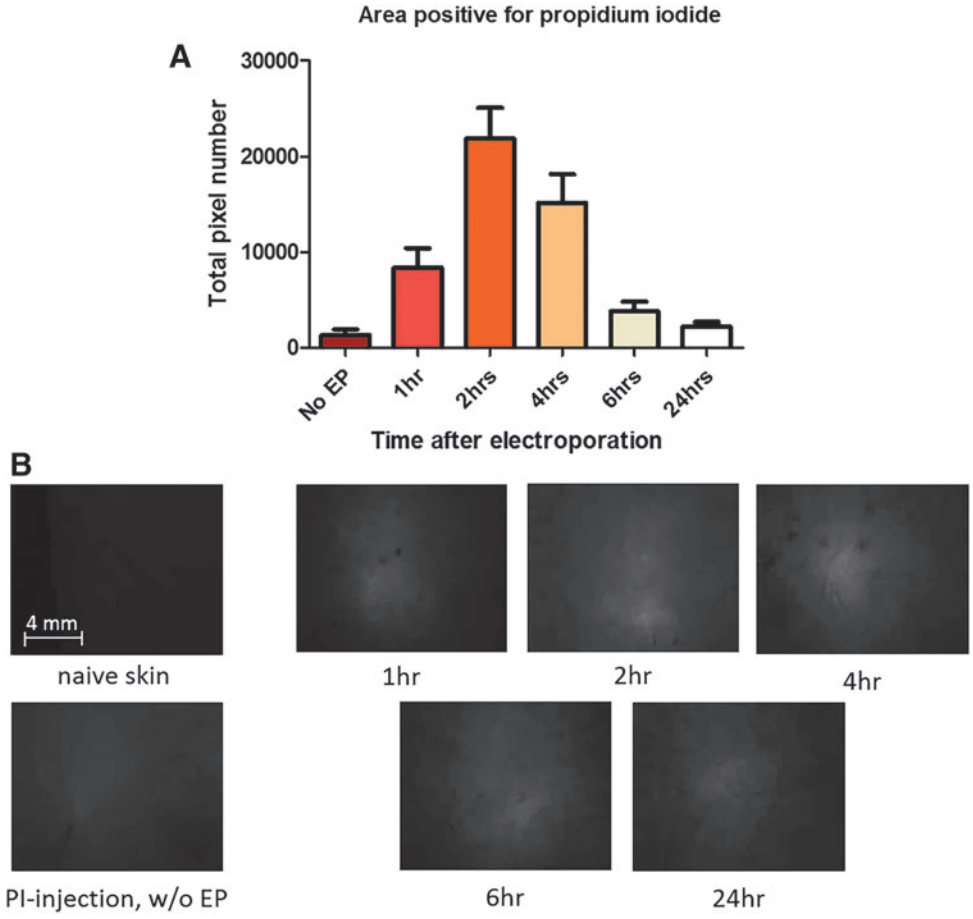

Figure 4. Dermal electroporation induces necrotic events. One hundred microliters of PBS was administered to guinea pig skin and the site was immediately electroporated. Propidium iodide (PI; 100 μL) was injected 20 minutes before skin collection. Pixel count analysis ($n=8$) of PI intensity at defined time points following electroporation (EP) treatment was graphed as pixel intensity **(A)**. Representative gross images of untreated, PI injection only, and electroporated skin surface 1, 2, 4, 6, and 24 hours posttreatment **(B)**.

is not due to passive diffusion of the fluorescent molecule into the cell through the pores created by EP as such pores are only present for a short period of time and would have resealed before the injection of PI.[23] In summary intradermal electroporation of the skin results in a rapid but brief occurrence of cell death (both apoptotic and necrotic in nature) at the site of treatment.

Distribution of dermal cell death at intradermal EP treatment site over a 24 h time period

With the aim of understanding the global level of cell death at the EP treatment site and whether this was related to the proximity of the insertion of the electrodes, we used fluorescent microscopy to observe apoptotic (Fig. 5) and necrotic (Fig. 6) events at 1, 2, 4, 6, and 24 h time points after EP. The cartoon (Figs. 5A and 6A) depicts the location of the skin areas 1 to 4 analyzed in relation to proximity to an electrode. By fluorescent microscopy imaging, we observed epidermal cells in close proximity to the insertion point of an electrode needle (within a 500 μm radius of the position of an electrode—panel 1 in Figs. 5A and 6A) were strongly impacted by the electroporation treatment. One hour after EP treatment, morphology of cell nuclei, as visible by staining of the skin section with DAPI, was altered (panel 1 of Figs. 5B and 6B). The nuclei in this region closest to the electrodes appear reduced in size and elongated. The majority of cells in the upper layers of the epidermis were TUNEL-positive 1 hour after EP treatment. By 4 hours after treatment, almost all nuclei in the entire strata of the epidermis close to an electrode needle were TUNEL-positive and appear smaller and with condensed DNA content. At time points 6 and 24 h after treatment there were fewer TUNEL-positive nuclei in the basal layer of the epidermis within close proximity to an electrode, and the morphology of the nuclei (following DAPI

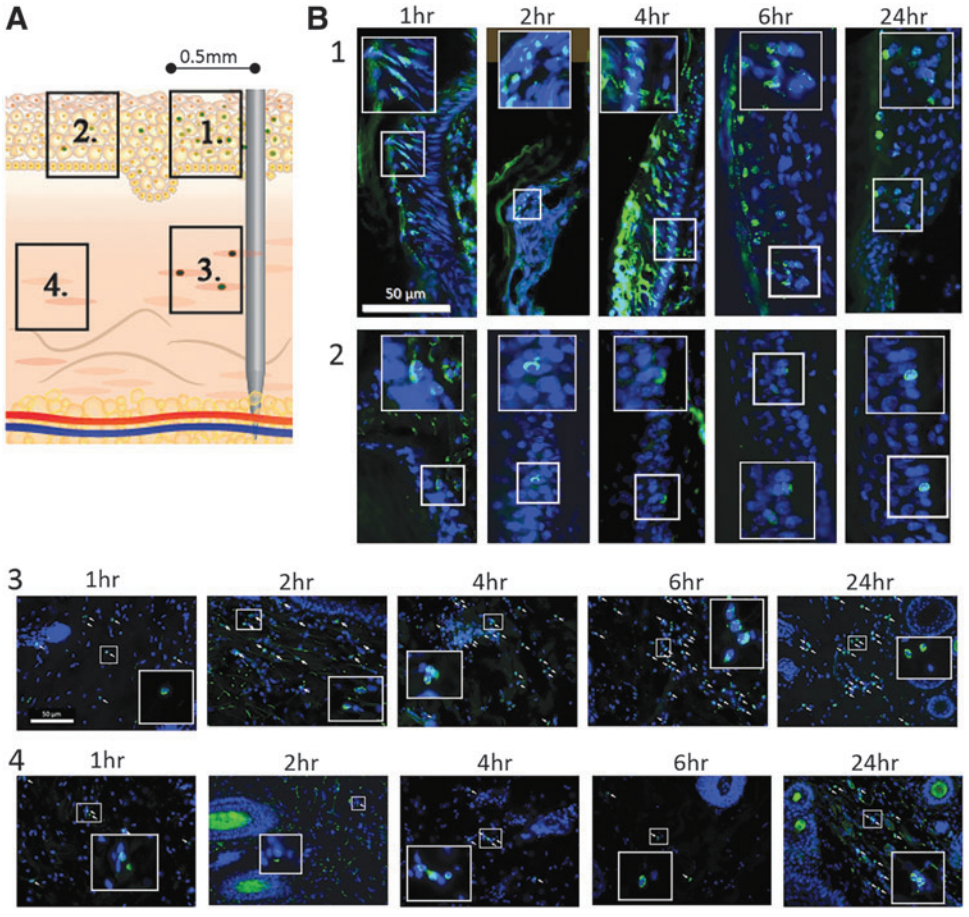

Figure 5. Distribution of apoptosis at dermal electroporation site across a 24 h time period. PBS (100 μL) was administered to guinea pig skin and the site was immediately electroporated. **(A)** Numbered regions identify location in the dermis in relation to an EP needle. **(B)** Skin was harvested at 1, 2, 4, 6, and 24 hours after treatment. Skin sections were stained using the TUNEL-assay (green) and DAPI counterstained (blue). Numbered panels refer to locations identified in (A). Images shown are single representations for sections obtained from five treatment sites. All panel insets are 8×magnification. White arrows identify TUNEL nuclei.

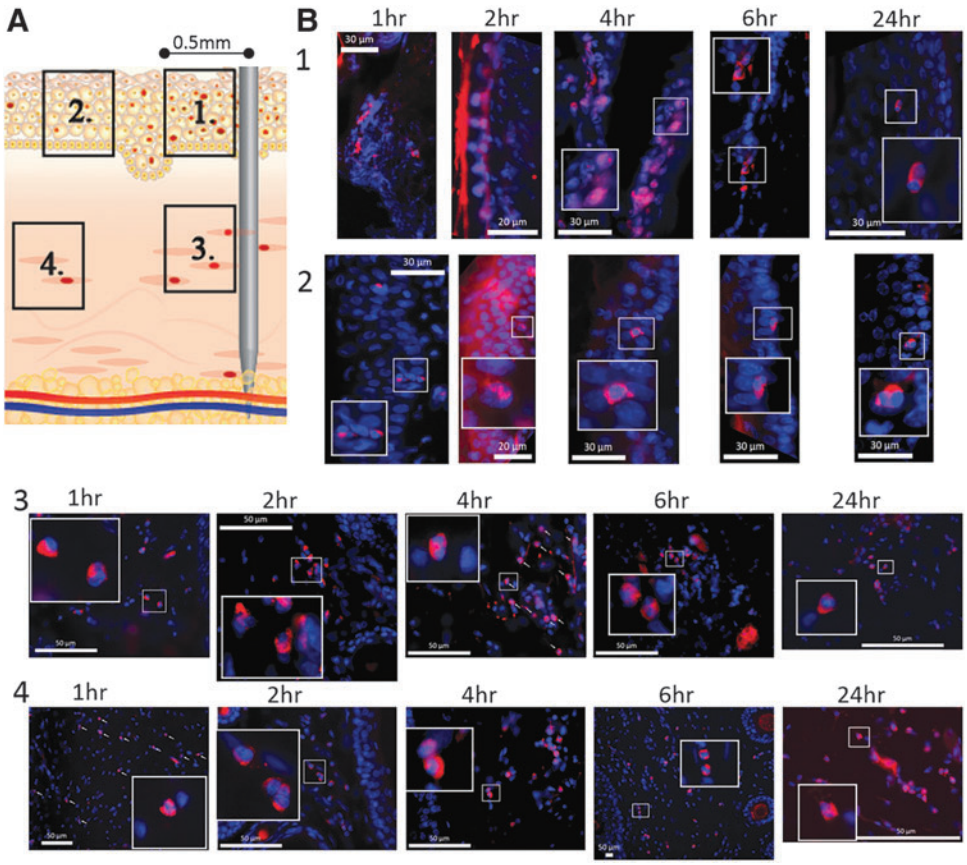

Figure 6. Distribution of necrosis at dermal electroporation site across a 24 h time period. PBS (100 μL) was administered to guinea pig skin and the site was immediately electroporated. At indicated time points after treatment, 100 μL PI was injected at the site and skin was harvested 20 minutes later. **(A)** Numbered panels refer to location in the dermis in relation to an EP-needle as indicated in the illustration. **(B)** Sections of treated guinea pig skin were stained with PI (red) and DAPI (blue) counterstained. Images shown are single representations for sections obtained from five treatment sites. All panel insets are 8×magnification. White arrows indicate PI-positive nuclei.

stain) appeared normal. Distal epidermal cells outside the 500 μm radius from an electrode (panel 2 in Figs. 5A and 6A), but still located within the area of the EP field, were impacted less than the cells within the radius. Apoptosis indicated by TUNEL-positive nuclei (Fig. 5B, panel 2) or necrotic cells (PI-positive nuclei Fig. 6B, panel 2) were rare and their frequency did not change within the examined 24 h time range after EP.

With regard to the kinetics of cell death following EP, apoptotic events in the dermis close to an electrode (panel 3 in Fig. 5A) can be observed as early as 1 h after treatment. The number of TUNEL-positive cells peaks at 6hr after EP treatment and was stable up to 24 h after treatment (Fig. 5B, panel 3). In electrode distant dermal areas (panel 4 in Fig. 5B), apoptosis was a rare event within 1 to 6 h of treatment. Twenty-four hours after the EP treatment, an increased number of TUNEL-positive nuclei can be observed in this region (Fig. 5B, panel 4). The morphological change of TUNEL-positive nuclei in the dermis was not as striking as the change observed in the epidermis after EP.

Necrosis was observed in the epidermis and was more prominent closer to the electrode needles (Fig. 6B, panels 1 and 2). Low numbers of PI-positive nuclei could be observed as early as 1 h after treatment, with their number peaking between 2 and 4 h, and decreasing between 6 and 24 h after the EP. These findings were in agreement with our previous observation showing the peak of PI in the skin close to the electrode at 2 h post EP (Fig. 4B). Necrotic events in the epidermal cells within the area of the EP field but more distant from electrode needles were less frequent. Necrotic cells can be detected at the 24 h time point but were rare and their frequency did not change over the time period analyzed.

Dermal calreticulin expression after ID Electroporation

The calcium-binding protein calreticulin is associated with a variety of intra- and extracellular

functions. In the endoplasmic reticulum it serves as a chaperone for glycoproteins and maintains intracellular calcium homeostasis. In the nucleus it modulates nuclear hormone receptor–regulated gene transcription. The translocation of calreticulin to the cell surface is a hallmark of immunogenic cell death. It was revealed that externalized calreticulin on apoptotic cells serves as an "eat-me" signal for dendritic cells and macrophages.[24] Recent studies have demonstrated that electric pulses stimulate the exposure of calreticulin *in vitro*.[25,26]

Here we show calreticulin to be up-regulated after *in vivo* EP in the skin (Fig. 7). In naïve skin, low calreticulin expression can be observed in the epidermis and the epithelial cells lining the hair follicles. Slightly increased levels were observed as early as one hour after EP treatment in the epidermis and follicular epithelium. The timing corresponded to early apoptotic events which we observed occurring one hour after EP (Figs. 3 and 5). At four to six hours after EP, calreticulin was highly increased in the epidermis and the follicular epithelium. Calreticulin was also significantly up-regulated in the dermis at this time. Unlike for TUNEL-positive cells, calreticulin expression was not closely localized to the electrode and appears to be more globally distributed throughout the EP field. The peak level of calreticulin coincides with the peak of cellular infiltration we observed six hours after EP (Fig. 2). Twenty-four hours after the EP treatment, calreticulin levels in epidermis and dermis had returned to background levels.

DISCUSSION

In vivo electroporation is widely employed to enhance gene expression in DNA vaccine and other gene-based protocols both in the preclinical and clinical setting. In this study we report on the inflammatory mechanisms initiated after EP using an intradermal electroporation device, the CELLECTRA®-3P, in the guinea pig skin. We show rapid induction of apoptosis and necrosis following EP treatment, with such events being intensified at the direct site of the penetrating electrodes. Additionally, we also detected infiltration of innate immune cells within hours of treatment. This fits with the established physiological response following a cell death event. Finally, we detected transient upregulation of the phagocyte "eat me" signal of calreticulin 4–6 h following EP treatment. As we will discuss below, these mechanisms may not be optimal for high levels of prolonged gene expression but may be advantageous to the aug-

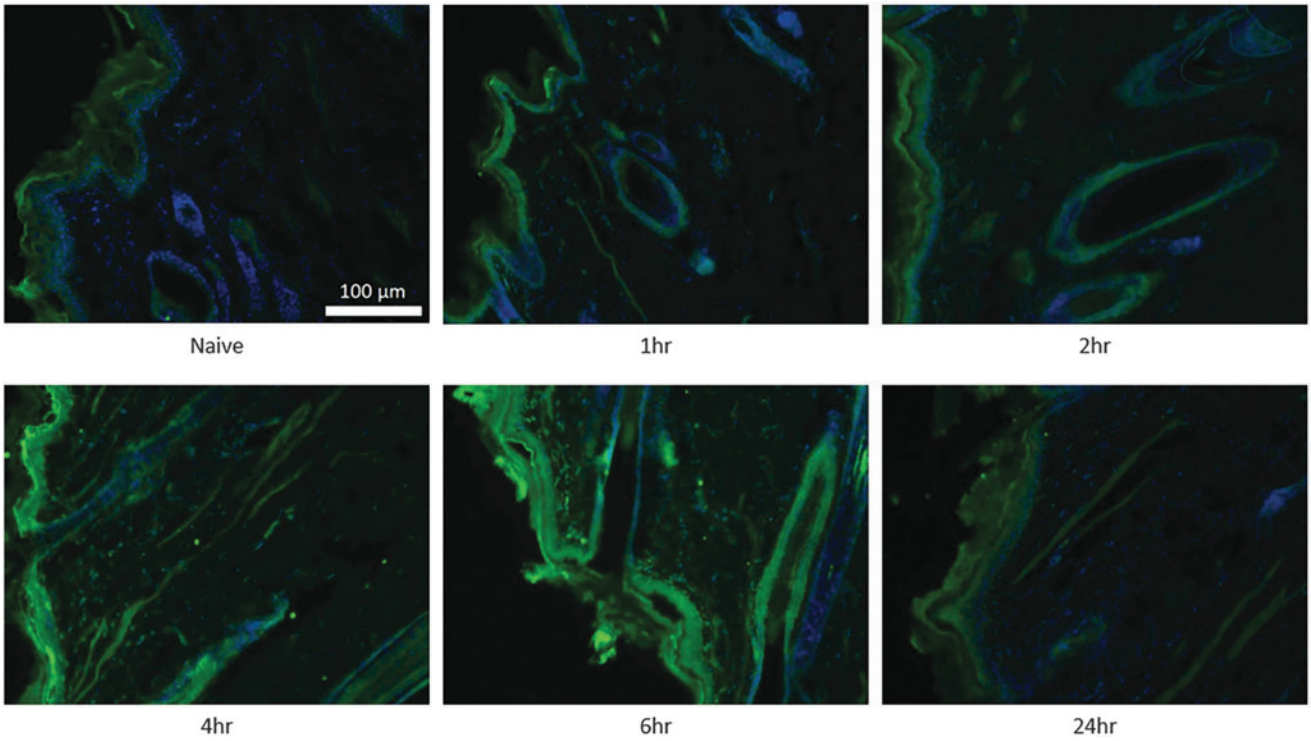

Figure 7. Kinetics of calreticulin expression after dermal electroporation. PBS (100 μL) was administered to guinea pig skin and the site was immediately electroporated. Skin samples were harvested at 1, 2, 4, 6, and 24 hours after treatment. Individual sections of naïve and treated skin were stained with an anti-calrecticulin antibody (Alexa Fluor 488, green) and DAPI (blue). Images shown are single representations for sections obtained from five treatment sites.

mentation of the host immune responses elicited by a vaccine delivered to the skin. We also discuss the balance which exists between inflammation in relation to gene expression and the type immune responses elicited. Finally, we discuss potential strategies to manipulate the level and quality of inflammation associated with EP with the goal of optimizing both the immune response generated and the tolerability of the procedure while not compromising gene expression.

Matzinger introduced the "danger theory" in 1994, it concerned the mechanisms by which apoptotic and necrotic cells could act as immunostimulants mediating productive immune responses by releasing signals.[27] These signals were termed damage-associated molecular patterns (DAMPs). Even though parts of the "danger theory" remain controversial, it is widely accepted that immunostimulatory danger signals are released and an inflammatory milieu is created after physical, biological, or chemical-mediated damage occurs in the tissue. Electroporation would be an example of physical damage to a tissue. Within this inflammatory milieu, antigen presenting cells are activated and acquire the ability to present antigen to the adaptive immune system in a manner which elicits productive T and B cell responses.[28–30] In our study, we have investigated the outcome in terms of cell death and innate immune cell infiltration and signaling that occurs after intradermal electroporation.

Initially, we demonstrated that intradermal EP resulted in infiltration of immune cells into the area surrounding the treatment site (Fig. 2). Following EP-enhanced pDNA delivery to the skin, we have identified a sub-population of the infiltrating cells to be macrophages (unpublished observations). Professional antigen presenting cells, such as macrophages and dendritic cells, can both capture the antigen secreted by transfected cells or engulf apoptotic cells. Cell death, whether it be via apoptosis or necrosis mechanisms, in an inflammatory milieu can have an adjuvant effect by the release of DAMPs and provide the antigenic material to be processed by local antigen presenting cells (APC), and subsequently presented to the adaptive immune system. In line with this, Depelsenaire *et al*. recently hypothesized that co-localized cell death serves as a "physical immune enhancer" in the context of nanopatch-delivered antigens to the skin.[31] We detected apoptotic events starting in the skin as early as one hour after EP treatment, with the most intense TUNEL staining observed at the 4 h time point (Figs. 3 and 5). Similar kinetics were reported for the necrotic events, with peak propidium iodide staining detected at 2 h post EP treatment (Figs. 4 and 6). Infiltration of inflammatory cells into the area surrounding the treatment site peaked at 6 h, and upregulated calreticulin expression was also observed at these early time points (Fig. 7). The kinetics of cell death, infiltration, and calreticulin signal are summarized in Table 1. The appearance of high levels of calreticulin is of particular interest to us. Calreticulin has been associated with immunogenic cell death of cancer cells.[32,33] Calreticulin enhances T-cell responses and antitumor effects to virus-antigen expressing tumors after DNA vaccination.[34] Furthermore, it was successfully used as adjuvant to increase humoral responses against SARS-Cov protein vaccine.[35] Cells expressing calreticulin on their surface may signal via CD91 to professional APCs to be engulfed. The cell associated antigens would be processed and presented in an immunogenic manner by the APC. This would lead to cross-presentation of tumor-associated antigens or vaccine-associated antigens. We are currently investigating the localization of calreticulin with pDNA vaccine-transfected cells expressing encoded antigens.

Table 1. *Kinetic summary of apoptotic and necrotic events in the skin after electroporation treatment*

	Time Post Electroporation Treatment				
	1 hr	*2 hr*	*4 hr*	*6 hr*	*24 hr*
Area 1	**	**	****	**	*
	+++	++++	++++	++	+
Area 2	*	*	*	*	*
	+	+	+	+	+
Area 3	*	**	***	****	****
	++	+++	++++	+++	++
Area 4	*	*	**	**	***
	++	++	++	++	+++
Infiltration	0	00	00	0000	000
Calreticulin	#	#	##	####	#

Scoring of necrosis (+) and apoptosis (*) in areas 1–4 of the skin (corresponding with panels in Figs. 5B and 6B) and cell infiltration (0; corresponding panels in Fig. 2) and calreticulin-signal (#; corresponding panels in Fig. 7) following electroporation treatment. Increase in number of symbols (1 to 4) correlates with increase in signal.

Previous studies have revealed reporter gene expression after EP-enhanced delivery at the skin within one hour.[7,17] It is interesting to speculate how these cell death mechanisms affect gene expression. Firstly, gene expression has been detected in both the epidermis and the dermis following intradermal EP. Interestingly, upon comparison of the levels of expression in the epidermis after CELLECTRA®-3P (invasive electrodes) and surface EP (noninvasive, surface contact electrodes), we have observed higher gene

expression in the epidermis using the latter delivery device.[36] Data reported here suggest the lower gene expression levels observed in the epidermis following CELLECTRA®-3P EP may be in part due to the increase in cell death events (both apoptotic and necrosis) induced by EP. On the other hand, the greater internal E-field generated by the CELLECTRA®-3P covers cells over a wider area than the surface EP device, permitting cells residing in the lower regions of the skin such as the dermis and subcutaneous region to be transfected. Thus we believe there is a balance between the associated cellular damage negatively impinging on gene expression around the immediate proximity of the electrodes, and the larger E-field produced by CELLECTRA®-3P permitting gene expression at more distal sites.

In summary, we believe that striking a balance between several EP-related factors (such as device design and EP parameters) could result in a beneficial impact of the elicitation of host immune responses to the delivered vaccine. High EP voltages lead to a larger E-field and permit a larger area of tissue to be transfected, additionally the local inflammation will aide to adjuvant the host immune response. However, voltages that are too high may cause increased levels of cell death and thus directly impinge on the ability of the tissue to express the desired pDNA encoded antigen. Furthermore, it is possible higher voltages may have a negative effect on tolerability of the procedure in the clinic. Thus, in summary, understanding the inflammatory mechanisms induced by intradermal EP delivery of gene-based therapeutics will enhance our ability to further tailor EP-based delivery protocols to drive the gene expression levels and immune responses desired.

ACKNOWLEDGMENTS

The authors thank Janess Mendoza and Lauren Jann for providing general laboratory operational support, Jay McCoy for support of the EP device, and Niranjan Sardesai for review of the manuscript and thoughtful advice. Finally, the authors thank the members of staff at BTS, Inc., for providing care for our laboratory animals.

AUTHOR DISCLOSURE

K.E.B., T.R.F.S., K.A.K., A.W., J.O. and K.S. are current employees of Inovio and as such have financial interest (in the form of salary compensation, stock options, and/or stock ownership) in the work described in this manuscript. W.B.K. has no potential conflicts of interest.

REFERENCES

1. Hickling JK, Jones KR, Friede M, et al. Intradermal delivery of vaccines: potential benefits and current challenges. Bull World Health Organ 2011;89:221–226.
2. Laddy DJ, Yan J, Khan AS, et al. Electroporation of synthetic DNA antigens offers protection in nonhuman primates challenged with highly pathogenic avian influenza virus. J Virol 2009;83: 4624–4630.
3. Shedlock DJ, Aviles J, Talbott KT, et al. Induction of broad cytotoxic T cells by protective DNA vaccination against Marburg and Ebola. Mol Ther 2013;21:1432–1444.
4. Cashman KA, Broderick KE, Wilkinson ER, et al. Enhanced efficacy of a codon-optimized DNA vaccine encoding the glycoprotein precursor gene of Lassa virus in a guinea pig disease model when delivered by dermal electroporation. Vaccines (Basel) 2013;1:262–277.
5. Hirao LA, Wu L, Khan AS, et al. Intradermal/subcutaneous immunization by electroporation improves plasmid vaccine delivery and potency in pigs and rhesus macaques. Vaccine 2008;26:440–448.
6. Kulkarni V, Rosati M, Bear J, et al. Comparison of intradermal and intramuscular delivery followed by in vivo electroporation of SIV Env DNA in macaques. Hum Vaccin Immunother 2013;9:2081–2094.
7. Smith TR, Schultheis K, Kiosses WB, et al. DNA vaccination strategy targets epidermal dendritic cells, initiating their migration and induction of a host immune response. Mol Ther Methods Clin Dev 2014;1:14054.
8. Roos AK, Moreno S, Leder C, et al. Enhancement of cellular immune response to a prostate cancer DNA vaccine by intradermal electroporation. Mol Ther 2006;13:320–327.
9. Donate A, Coppola D, Cruz Y, et al. Evaluation of a novel non-penetrating electrode for use in DNA vaccination. PLoS One 2011;6:e19181.
10. El-Kamary SS, Billington M, Deitz S, et al. Safety and tolerability of the Easy Vax clinical epidermal electroporation system in healthy adults. Mol Ther 2012;20:214–220.
11. Hutnick NA, Myles DJ, Ferraro B, et al. Intradermal DNA vaccination enhanced by low-current electroporation improves antigen expression and induces robust cellular and humoral immune responses. Hum Gene Ther 2012;23:943–950.
12. Laddy DJ, Yan J, Kutzler M, et al. Heterosubtypic protection against pathogenic human and avian influenza viruses via in vivo electroporation of synthetic consensus DNA antigens. PLoS One 2008;3:e2517.
13. Diehl MC, Lee JC, Daniels SE, et al. Tolerability of intramuscular and intradermal delivery by CELLECTRA((R)) adaptive constant current electroporation device in healthy volunteers. Hum Vaccin Immunother 2013;9:2246–2252.
14. Sardesai NY, Weiner DB. Electroporation Delivery of DNA Vaccines: Prospects for Success. Current opinion in immunology 2011;23:421–429.
15. Gehl J, Sorensen TH, Nielsen K, et al. In vivo electroporation of skeletal muscle: threshold, efficacy and relation to electric field distribution. Biochim Biophys Acta 1999;1428(2–3): 233–240.
16. Babiuk S, Baca-Estrada ME, Foldvari M, et al. Increased gene expression and inflammatory cell infiltration caused by electroporation are both

important for improving the efficacy of DNA vaccines. J Biotechnol 2004;110:1–10.

17. Amante DH, Smith TR, Mendoza JM, et al. Skin Transfection Patterns and Expression Kinetics of Electroporation-Enhanced Plasmid Delivery Using the CELLECTRA-3P, a Portable Next-Generation Dermal Electroporation Device. Hum Gene Ther Methods 2015;26:134–146.
18. Ito WD, Schaarschmidt S, Klask R, et al. Infarct size measurement by triphenyltetrazolium chloride staining versus in vivo injection of propidium iodide. J Mol Cell Cardiol 1997;29:2169–2175.
19. Wolff RA, Chien GL, van Winkle DM. Propidium iodide compares favorably with histology and triphenyl tetrazolium chloride in the assessment of experimentally-induced infarct size. J Mol Cell Cardiol 2000;32:225–232.
20. Bahmani P, Schellenberger E, Klohs J, et al. Visualization of cell death in mice with focal cerebral ischemia using fluorescent annexin A5, propidium iodide, and TUNEL staining. J Cereb Blood Flow Metab 2011;31:1311–1320.
21. Boissonnas A, Fetler L, Zeelenberg IS, et al. In vivo imaging of cytotoxic T cell infiltration and elimination of a solid tumor. J Exp Med 2007;204:345–356.
22. Carpenter AE, Jones TR, Lamprecht MR, et al. CellProfiler: image analysis software for identifying and quantifying cell phenotypes. Genome biology 2006;7:R100.
23. Krassowska W, Filev PD. Modeling Electroporation in a single cell. Biophys J 2007;92:404–417.
24. Gardai SJ, McPhillips KA, Frasch SC, et al. Cell-surface calreticulin initiates clearance of viable or apoptotic cells through trans-activation of LRP on the phagocyte. Cell 2005;123:321–334.
25. Calvet CY, Famin D, Andre FM, et al. Electrochemotherapy with bleomycin induces hallmarks of immunogenic cell death in murine colon cancer cells. Oncoimmunology 2014;3:e28131.
26. Nuccitelli R, Berridge JC, Mallon Z, et al. Nanoelectroablation of Murine Tumors Triggers a CD8-Dependent Inhibition of Secondary Tumor Growth. PLoS one 2015;10:e0134364.
27. Matzinger P. Tolerance, danger, and the extended family. Annu Rev Immunol 1994;12:991–1045.
28. Banchereau J, Steinman RM. Dendritic cells and the control of immunity. Nature 1998;392:245–252.
29. He Y, Zhang J, Donahue C, et al. Skin-derived dendritic cells induce potent CD8(+) T cell immunity in recombinant lentivector-mediated genetic immunization. Immunity 2006;24:643–656.
30. Heath WR, Belz GT, Behrens GM, et al. Cross-presentation, dendritic cell subsets, and the generation of immunity to cellular antigens. Immunol Rev 2004;199:9–26.
31. Depelsenaire AC, Meliga SC, McNeilly CL, et al. Colocalization of cell death with antigen deposition in skin enhances vaccine immunogenicity. J Invest Dermatol 2014;134:2361–2370.
32. Obeid M, Tesniere A, Ghiringhelli F, et al. Calreticulin exposure dictates the immunogenicity of cancer cell death. Nat Med 2007;13:54–61.
33. Panaretakis T, Kepp O, Brockmeier U, et al. Mechanisms of pre-apoptotic calreticulin exposure in immunogenic cell death. EMBO J 2009;28:578–590.
34. Yang B, Yang A, Peng S, et al. Co-administration with DNA encoding papillomavirus capsid proteins enhances the antitumor effects generated by therapeutic HPV DNA vaccination. Cell Biosci 2015;5:35.
35. Qiu X, Hong C, Li Y, et al. Calreticulin as a hydrophilic chimeric molecular adjuvant enhances IgG responses to the spike protein of severe acute respiratory syndrome coronavirus. Microbiol Immunol 2012;56:554–561.
36. Mendoza JM, Amante DH, Kichaev G, et al. Elucidating the kinetics of expression and immune cell infiltration resulting from plasmid gene delivery enhanced by surface dermal electroporation. Vaccines (Basel) 2013;1:384–397.

Received for publication November 2, 2017;
accepted after revision June 25, 2018.

Published online: June 27, 2018.